

Preface

Micro injection molding is the preferred process technology for the mass production of polymer micro components. Micro molded parts are characterized by dimensional tolerances in the micrometer range, high surface finish in the sub-micrometer down to optical range, and high geometrical complexity. Micro injection molding is used to manufacture highly valued micro medical components (sensors, implants, tubes, catheter tips), micro optics, microfluidic systems, and micro mechanical systems, among others. The global market of micro injection molding is expected to reach USD 1 billion by 2020 with a compound annual growth rate between 10–15% in the period 2013–2020. High demand for micro molded parts is seen from the medical, healthcare, automotive, and electronics sectors.

To exploit the micro molding technology process capabilities and take advantage of research and market opportunities, there was a need for a dedicated book that deals exclusively with micro injection molding and the knowledge to overcome the challenges of successfully managing and processing polymer materials at these ultra-small scales. This book meets that need. Micro injection molding is indeed not just a simple downscaling of conventional injection molding, and specific material-process-product interactions must be understood in order to achieve near zero-defect net-shape micro molded products.


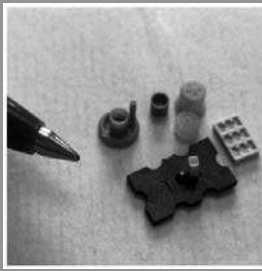
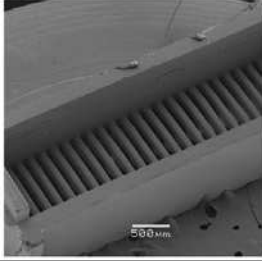
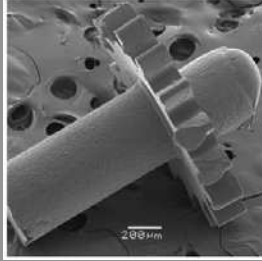
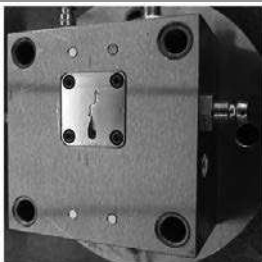
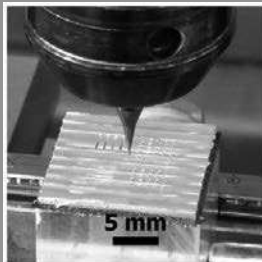
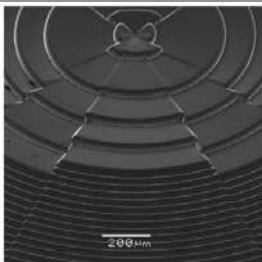
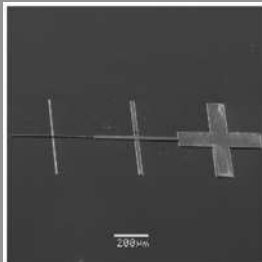
“Micro Injection Molding” is written for engineers, researchers, project managers, consultants, and other professionals involved in precision polymer processing and micro manufacturing. The book provides a comprehensive, up-to-date, and detailed treatment of the main topics related to micro molding. It includes the underlying physics of micro polymer processing and replication at the micro/nano scales, as well as fundamentals of micro molding machine construction and tool making technologies (micro machining, surface treatments). The book also discusses in detail supporting technologies for high-precision micro molding such as quality control of micro parts, micro additive manufacturing for micro product prototyping, and process simulation. Process variations such as vacuum-assisted micro molding and multimaterial processing (micro two-component injection molding,

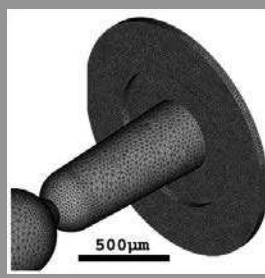
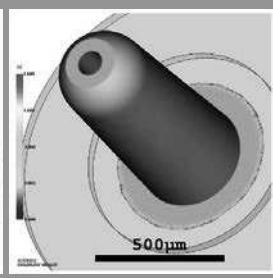
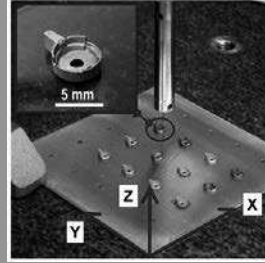
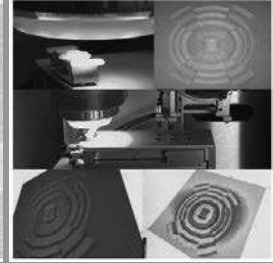
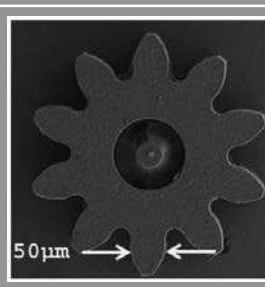
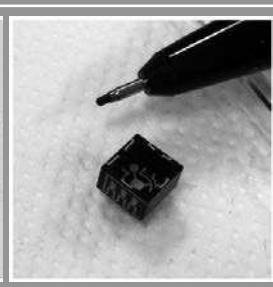
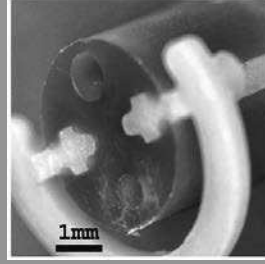
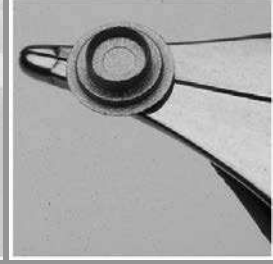
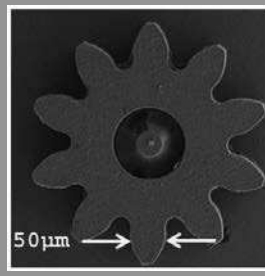
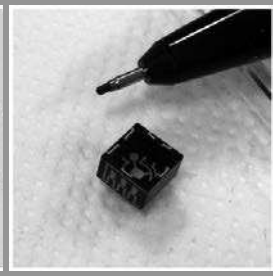
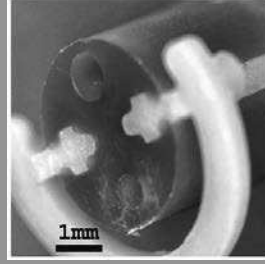
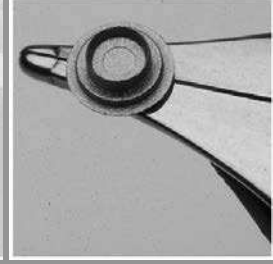
metal and ceramic micro molding) bringing further opportunities for advanced micro manufacturing are presented in detail as well.

The book is composed of 13 chapters organized in four parts (see table below):

- Part 1 - Polymer Materials and Process Micro Technology
- Part 2 - Tooling Technologies for Micro Mold Making
- Part 3 - Micro Molding Key-Enabling Technologies
- Part 4 - Multimaterial Micro Processing

“Micro Injection Molding” Book Chapters Organized in Four Parts

Part	Chapters	Illustrations
1. Polymer Materials and Process Micro Technology	1. Micro Injection Molding Machines Technology	   
	2. Micro Molding Process Monitoring and Control	
	3. Polymer Materials Structure and Properties in Micro Injection Molding Parts	
	4. Surface Replication in Micro Injection Molding	
2. Tooling Technologies for Micro Mold Making	5. Micro Machining Technologies for Micro Injection Mold Making	   
	6. Ultra-Precision Machining Technologies for Micro Injection Mold Making	
	7. Surface Treatment of Mold Tools in Micro Injection Molding	

<p>3. Micro Molding Key-Enabling Technologies</p>	<p>8. Vacuum-Assisted Micro Injection Molding</p>		
	<p>9. Modeling and Simulation of Micro Injection Molding</p>		
	<p>10. Metrological Quality Assurance in Micro Injection Molding</p>		
	<p>11. Additive Manufacturing for Micro Tooling and Micro Part Rapid Prototyping</p>		
<p>4. Multi-material Micro Processing</p>	<p>12. Micro Powder Injection Molding</p>		
	<p>13. Multimaterial Micro Injection Molding</p>		

About the Author



Guido Tosello, PhD, is Associate Professor at the Technical University of Denmark, Department of Mechanical Engineering, Section of Manufacturing Engineering. He is senior lecturer, research manager, supervisor of PhD, MSc, and BSc projects, and industrial and management consultant. Guido's principal research interests are the analysis, characterization, monitoring, control, optimization, and simulation of precision molding processes at micro/nano scales of thermoplastic materials.

Technologies supporting precision/micro/nano molding processes are of research interest, for example: advanced process chain for micro/nano tools manufacturing, quantitative validation of injection molding simulation, additive manufacturing, dimensional and surface micro/nano metrology, measurement calibration and uncertainty, statistical process control, design of experiment, polymer materials characterization, design and manufacture of 3D precision/micro components and micro/nano structured surfaces, and multimaterial and micro insert molding.

Guido Tosello is the recipient of the "Technical University of Denmark Best PhD Research Work 2008 Prize" for his PhD thesis "Precision Moulding of Polymer Micro Components"; of the 2012 Alan Glanvill Award by The Institute of Materials, Minerals and Mining (IOM3) (UK), given as recognition for research of particular merit in the field of polymeric materials; of the Young Research Award 2014 from the Polymer Processing Society (USA), in recognition of scientific achievements and research excellence in polymer processing within six years from PhD graduation; and of the Outstanding Reviewer Award 2016 of the Institute of Physics (UK) for his contribution to the Journal of Microengineering and Micromechanics.

- Identification of the key features performing each function: The performance (namely the level of the flows) of each function is due to a subset of features directly linked to it through causal chains.
- Analysis of the functional map: The map describing the machine can be used to highlight the negative function and those functions that are in contradiction. This is the main step of the procedure to investigate the failures and the useless functions performed by the machine.

After the functional analysis of the two machines is performed, a further step regarding the comparative analysis of the two functional maps is introduced. The comparison is also carried out by means of quality parameter measures obtained from actual experiments with both the injection and the micro injection molding machines. From the comparative analysis it will be possible to see how the maps describing the two different machines share some common patterns but also have different functional sequences. The analysis of the differences between the two functional maps allows for a direct correlation between functional design reasons and different performances. The analysis of differences can produce hypotheses for machine redesign.

1.3.3 Functional Analysis

The micro injection molding process operated with two different machines (a conventional injection molding machine and a micro injection molding machine) has been studied and compared in order to fully understand the reasons of their design and to correlate design choices and final results (positive features as well as drawbacks and failures).

The following two different machines have been studied and compared:

- A small injection molding machine based on the conventional injection molding technology using the reciprocating plastication screw [28]. This machine is interesting, since it is an example of simple downscaling of the components, not a machine properly designed to manufacture micro parts.
- Micro injection molding machine with two pistons and a plastication screw [29–31]. The machine has an innovative design and its architecture seems to better meet the requirements for manufacturing micro parts through the injection molding process.

Process Phases

In order to identify all the functions of the machine, it is necessary to consider the various phases that occur during the process. Therefore, the study of the evolution of the flows leads to the determination of the transitions from one state to another, while homogenous sets of states represent phases. Following this approach, the

main phases of the micro injection process, described in the literature, are identified and summarized in Figure 1.6.

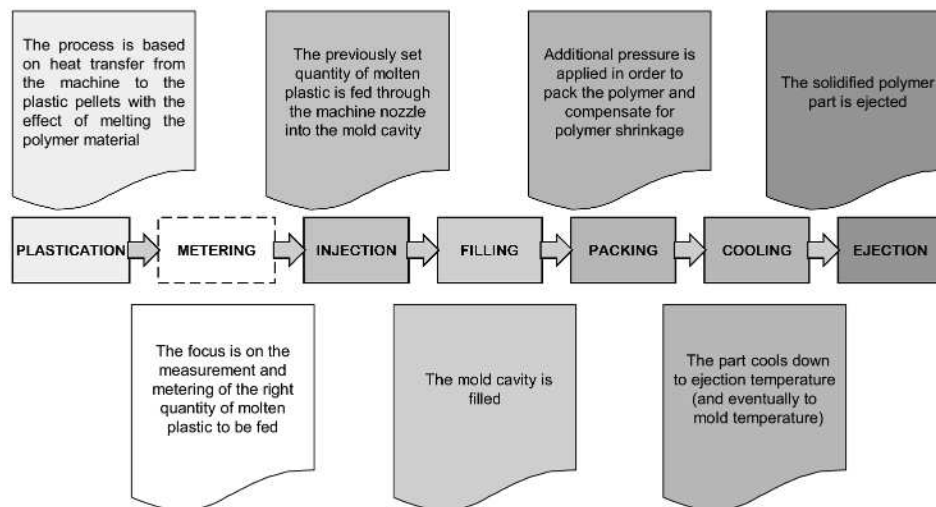


Figure 1.6 The main phases in the injection and micro injection molding processes

Figure 1.6 shows the main phases in the injection and micro injection molding processes (the dotted line block is absent in conventional injection machines, and present in micro molding machines).

It is worth noticing that the metering phase is explicitly described only in the machine with a screw and two pistons, and it is made possible by the control of a suitable valve. Conversely, in the conventional injection molding machine, as it will be shown more clearly in the next subsection, the metering phase is embedded in the contiguous phases.

Although the standard phases are those described above, according with the definition of phase given above, a more detailed process workflow is proposed (see Figure 1.7).

Actually, even from a quick analysis of the phases it is possible to notice that a new chain of functions related to the metering of the right amount of material has been introduced. On the other hand, the “screw’s setting” phase, which contained the metering in the traditional machine, is eliminated.

The detailed functional analysis shows the consequences coming from the introduction/elimination of some phases in the micro injection molding machine with two pistons and one screw.

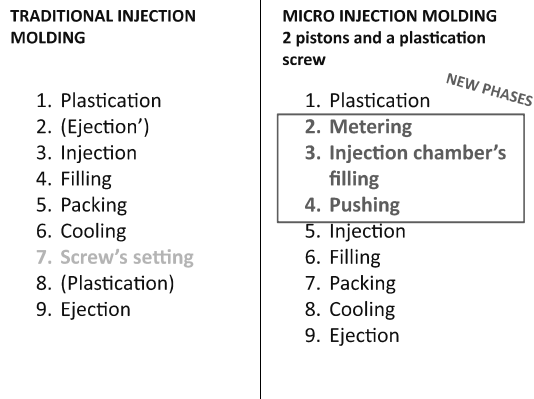


Figure 1.7 The different phases of conventional and micro injection molding processes

Functional Analysis of the Machines

After the identification of the phase of usage, the functional analysis of the two injection molding machines can be performed.

Each machine and its related detailed process are described in natural language. The functional description has been tagged as follows: bold for verbs and italic for flows, respectively.

Firstly, a conventional plastication-screw injection molding machine (see Figure 1.8) adapted for micro parts injection has been studied and analyzed. The machine and related detailed process have been described in natural language.

Structural description: A conventional injection molding machine (e.g., screw diameter = 15 to 18 mm, clamping force = 250–350 kN, maximum injection speed = 100–150 mm/s) can be adapted for manufacturing micro parts. An injection molding machine consists of a material hopper, an injection ram or screw-type plunger, and a heating unit. Injection molding machines hold the molds in which the components are shaped. Injection molding machines are rated by tonnage, which expresses the amount of clamping force that the machine can exert. This force keeps the mold closed during the injection process [28].

Functional description in natural language: First of all, *pellets moved by gravity* are **fed** to the *screw system*; during the plastication phase, the *screw* is **rotating** to build up the *melt polymer* necessary for the injection phase. The *volume* close to the tip of the screw is **heated** by *electrical units* and the *pellets* **melt**. During the rotation, the *molten polymer* is **fed** downward. The pressure **pushes** the *screw* backward. When sufficient *polymer* has built up (i. e., shot volume is plasticated), rotation **stops**; when the *mold* is **closed**, the *screw* is **pushed** (injection), the *melt polymer* **fills** the *sprue*, the *runners*, and the mold *cavity* (filling), and the *screw*

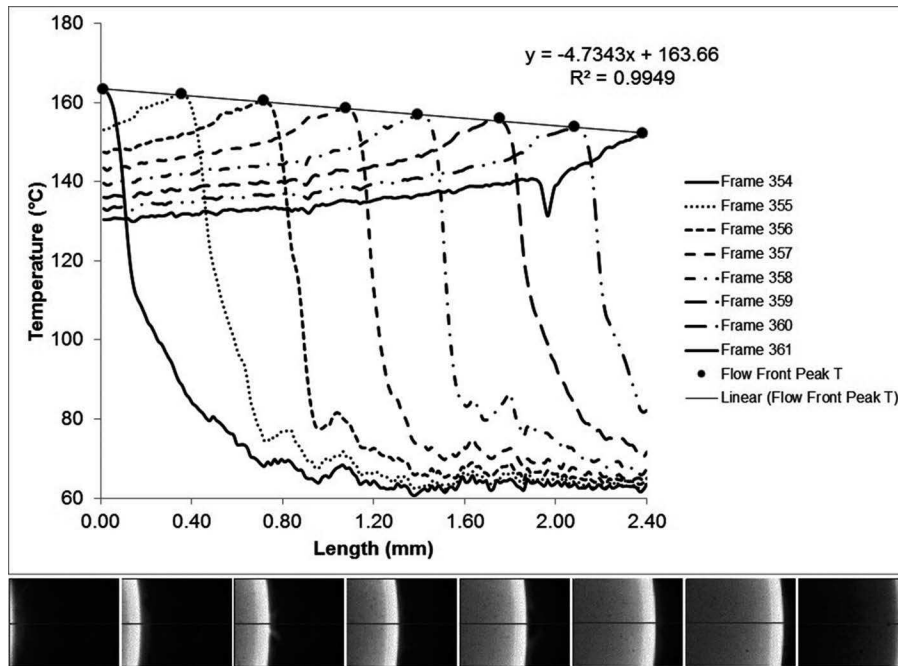


Figure 2.13 Flow front temperature measurements recorded during the filling of a disc component with a thickness of 500 μm

2.5.4 Simulation Boundary Conditions and Validation of Results

It is common to see cases where simulation software has been used to model a process and has failed to provide an accurate prediction of the mold filling behavior simply because incorrect boundary condition data has been used in the analysis. Common mistakes that are made are the use of melt and mold set temperature values (rather than those actually measured on the machine) and the use of default injection rates. Process monitoring systems allow these values to be measured directly to feed into the simulation model in order to create a more accurate model of the filling performance [19, 20]. The use of process monitoring tools allows understanding of systematic errors between set and actual values that can be used to improve the accuracy of future simulations.

These techniques can also be adopted to significantly improve less well-understood boundary conditions. A key parameter for determining the cooling behavior of a molding process is the heat transfer coefficient (HTC), which determines the flow of heat at the interface between the polymer and the mold tool. Small changes to this value can cause very large differences in simulation outcomes for micro molding processes, due to the very high surface to volume ratio of the components and

the very rapid cooling times. Work has been performed using a thermal imaging system to quantify the HTC value for a micro molding process and it can be seen that the default values do not provide an accurate description of the cooling behavior of the polymer at the interface, as shown in Figure 2.14. However, by applying values derived from the cooling curves recorded using the camera system, a much better fit is seen.

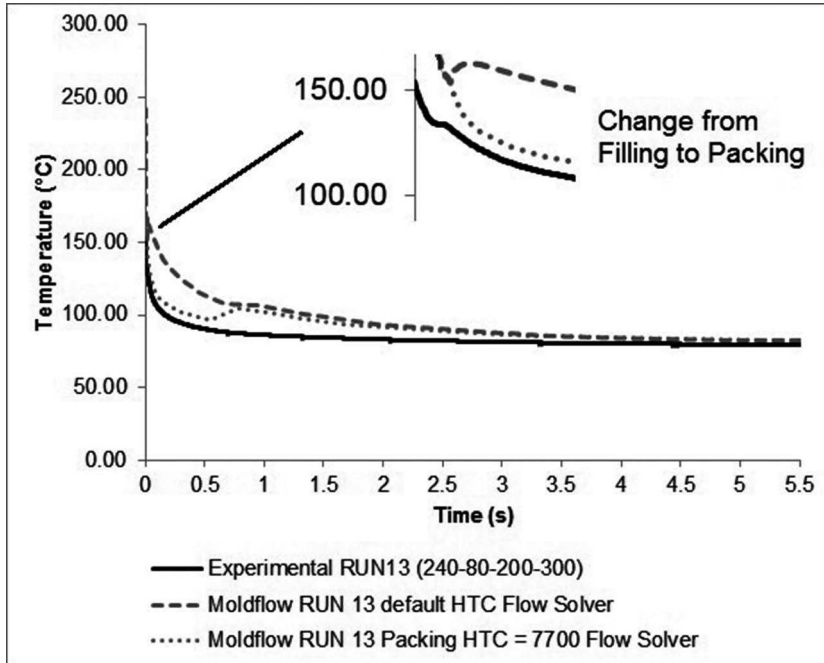


Figure 2.14 Comparison of simulated and experimental cooling curves describing component surface temperature

2.5.5 Sensor Development and Validation

Multiple sensor-based systems can be used to benchmark development sensor performance and also provide further understanding of the process environment [21]. The use of a common external clock signal to trigger the acquisition of each measurement sequentially allows data to be collected from multiple sources at the same point in time, allowing them to be directly compared. To illustrate this, Figure 2.15 shows the data collected using a Kistler 9211 sensor for injection pressure measurement, combined with a sequence of images acquired with a Mikrotron MC1310 high-speed camera, which were acquired synchronously. The increase in the pressure recorded by the sensor can be directly compared with the

flow front position at that time, providing greater insight into the process and providing useful information that could be used to directly determine flow behavior from pressure curves alone.

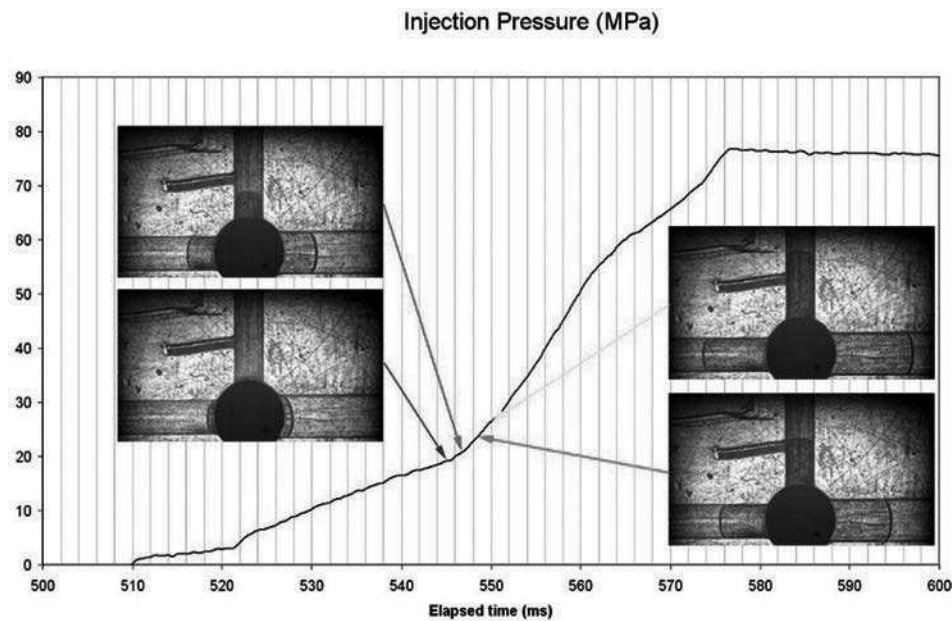


Figure 2.15 Synchronous injection pressure data and high-speed camera images of filling of a component with three channels of width 1.0, 1.5, and 2.0 mm

A second example is shown in Figure 2.16, where the recorded values of the amplitude for the reflection of ultrasonic waves generated using the piezoelectric film sensors described in Section 2.2.4 are synchronized with another high-speed camera visualization using a Mikrotron MC1310 camera. Here it can be seen that the amplitude of the reflection drops when the polymer enters the cavity, as some of the energy is transmitted into the polymer. As the part cools, the polymer detaches from the wall, causing the amplitude to return to the same level as when the cavity was empty.

■ 4.4 Influence of Tooling and Process Parameters on Replication of Microstructures

The possibility of processing polymer materials with technologies enabling large-volume production introduces solutions to remove the technology barrier between lab-scale proof-of-principle and the high-volume low-cost production of micro- and nano-technology-based products. In the previous sections, methods and approaches to process chain validation for final polymer micro and nano structure replication have been presented. In the following sections, the replication fidelity between different process chain steps and their dependency on process variation, process conditions, tool accuracy, material behavior, and features' geometries are considered and quantified.

4.4.1 Replication and Optimization of Deterministic Structures

The replication fidelity of deterministic geometries over the entire process chain can be quantified through traceable measurements on designed fingerprint test structures. To assess the critical factors affecting the replication quality throughout the different steps of the proposed process chain, test geometries are designed and produced on the side of the functional features. The so-called fingerprints of the lithography and molding processes are evaluated using atomic force microscopy. The entire process chain is therefore characterized and the degree of replication among the different replication steps quantified with precise measurements using a high accuracy relocation technique on the produced key test geometries [50].

The master geometries used in the presented study were fabricated as described in Section 4.2.1. Test geometries were composed of three crosses with a constant height (nominal design value equal to 62 nm) with horizontal and vertical wings with widths of 10 μm , 2 μm , and 500 nm, respectively. The crosses were positioned in the center of the produced 22 mm \times 22 mm nickel insert, which was used for the injection molding of approximately 1000 parts at the end of the experimental test procedure.

Micro/nano crosses polymer replicas were produced by injection molding (Figure 4.14) using a commercially available cyclic olefin copolymer (COC), Topas 6013.

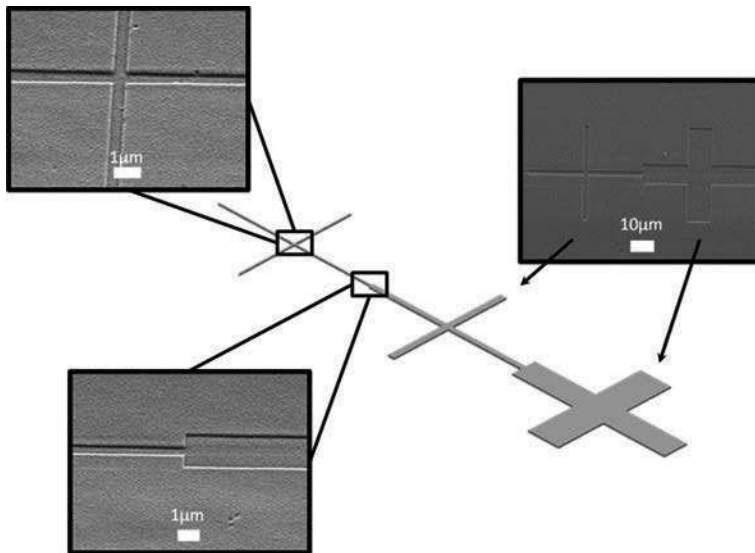


Figure 4.14 Scanning electron microscopy images of a COC molded part. The illustration shows the corresponding polymer replica details of the produced nickel micro/nano crosses

To evaluate the influence of process parameters on the replication of nano-scale structured surfaces, a statistically designed set of experiments was carried out [50]. The investigation was aimed at quantifying and optimizing the replication quality from the master geometry to the thermoplastic substrate on the parallel and perpendicular relative directions of the different cross wings with respect to the polymer flow.

At this dimensional scale, variations of the degree of replication due to replication process conditions, tool accuracy, material behavior, and feature geometry are in the order of a few micrometers down to a few tens of nanometers [3]. For this reason, high resolution AFM measurements are employed to assess and quantify the replication quality of the produced micro-nano crosses over the different substrates. Replication quality as a variation of H_{dev} (Eq. (4.1)) during the entire experimental plan is used as the output of the statistical analysis.

The results show the influence of both process parameters (mold temperature, packing time, packing pressure) and design parameters (channel width and direction with respect to the polymer flow) on the replication fidelity of the micro/sub- μm channels, providing effective guidelines for process and part design of injection molded microfluidic systems. It has been verified that a combination of high mold temperature and longer packing time improve the replication fidelity from the master to the polymer part. Moreover, results from the design of experiments have shown an improved process capability on replicating cross wings parallel to the polymer flow direction.

Measurement relocation was ensured by measuring with AFM the test structures on the three different substrates (Figure 4.15).

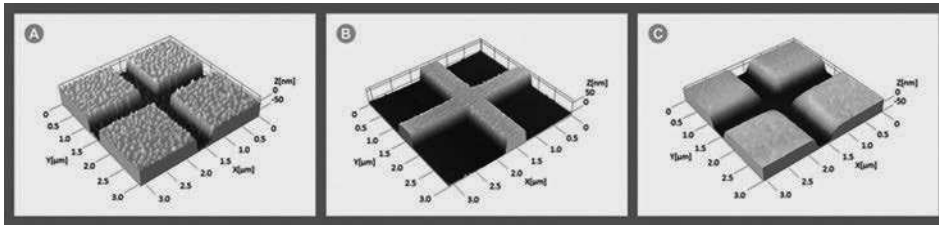


Figure 4.15 Process chain validation for sub-micro channel (width = 500 nm, depth = 60 nm) manufacture: (A) e-beam lithography on silicon, (B) nickel electroplating, (C) replication by micro injection molding (material: cyclic olefin copolymer, COC, TOPAS r 6013). Measurements by calibrated AFM measurements with uncertainty and relocation accuracy at nanometer level (magnification: X 1 ×, Y 1 ×, Z 5 ×)

A quantitative evaluation of the replication fidelity was performed considering the verification of dimensional tolerances with particular attention to the challenge of obtaining low measuring uncertainties [50].

An investigation into the crosses wings with different aspect ratios (1/161; 1/32; 1/8) shows the replication quality within the tolerance verification range. The average electroplated nickel trenches height among the three produced crosses is 98% of the average value of the corresponding etched grooves in the silicon wafer. The investigation helps, also, in understanding the process capability in terms of replication fidelity variation on the polymer substrate. The largest depth deviation was measured for cross number 3 with the smallest nominal width dimension of 500 nm. For an average measured polymer channel depth corresponding to 94% replication of the corresponding nickel trenches, a standard deviation of 4% among the smallest polymer crosses' depth was assessed.

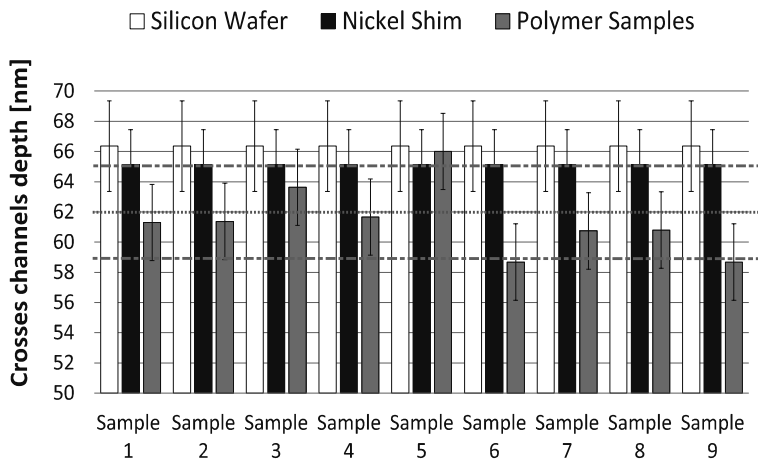


Figure 4.16 Quality control results of micro injection molded cross with nominal width of 500 nm. The square dot line represents the target design dimension of the crosses' height; the dash dot lines represent the tolerance range (as $\pm 5\%$ of the crosses' target design height). Histogram columns represent the channel depths measured on the silicon wafer ($U = 3.0$ nm), the nickel insert ($U = 2.3$ nm), and the polymer substrate ($U = 2.5$ nm). Error bars on the histogram columns indicate expanded combined uncertainty U ($k = 2$, conf. level 95%)

4.4.2 Replication Quality of Large Area Nano-Structured Surfaces

The establishment of periodic nanometer features can affect the physical (e. g., wetting behavior, hydrophobic/hydrophilic/self-cleaning properties) and optical properties (e. g., reflectivity) of a surface.

In order to understand the capability of micro injection molding on replicating periodical nanometer structures, the nickel insert produced as described in Section 4.2.2 was used. Three different thermoplastic materials were molded during the experimental phase (COC, PC, and PP).

In this example, the structured nickel insert area was $80 \text{ mm} \times 30 \text{ mm}$, and the typical single feature critical dimensions were, approximately, a diameter equal to 500 nm and height of 60 nm. Due to the extremely high number of nano features, a method based on the exact measuring repositioning able to compare measurements of corresponding features on the master and polymer surfaces could not be applied. Following the material supplier specifications, different process parameters were chosen to produce parts with different polymer materials. At the end of the experimental phase, in order to qualitatively characterize the achieved replication fidelity on the different polymer substrates, SEM pictures were captured. Images were taken in the same positions in an attempt to compare the polymer's properties with the replication obtained. On the sidewall and the bottom position of the fabricated micro-rectangular geometry, images were recorded to understand

replication behaviors which are otherwise difficult to characterize with conventional AFM measurements or conventional optical systems.

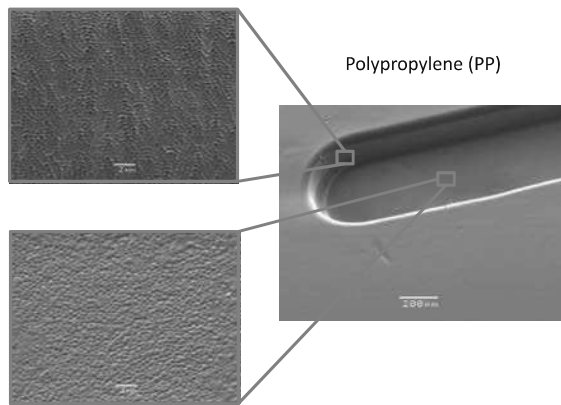


Figure 4.17 SEM pictures of replicated polymer surfaces

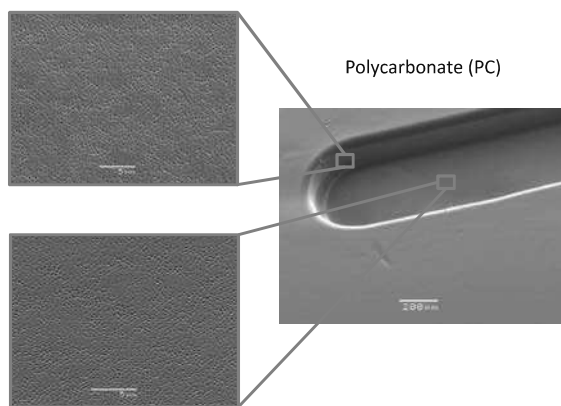


Figure 4.18 SEM pictures of replicated polymer surfaces

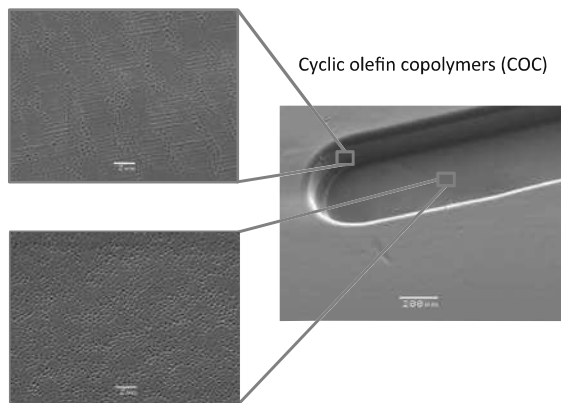


Figure 4.19 SEM pictures of replicated polymer surfaces

■ 6.2 Diamond Machining

6.2.1 Diamond Turning

In diamond turning processes, the cutting motion is provided by the rotating workpiece, while the tool is moved in relation to the surface, thereby copying the geometry of the diamond tool into the surface to determine the shape of the desired part. In the most basic set-up, only two controlled axes (for generating the feed and infeed motion) and a spindle are necessary for the generation of plane and rotationally symmetric surfaces or structures, such as Fresnel lenses. Diamond turning can also be used for on-axis, symmetrical part geometries, such as spherical shapes, but also for off-axis geometries with an asymmetrical design, i. e., aspheric mirrors like parabolic or elliptical surfaces.

The structure's shape can either be determined by the geometry of the diamond tool (profile-turning) or by modulation of the infeed depth (form-turning). Profile-turning can generate circular or spiral-type structures by plunging the diamond tool into the surface according to the radial position of the tool on the surface (Figure 6.2a) or by superposition of the tool geometry and the applied feed (Figure 6.2b). More complex shapes can be generated when contouring the desired shape by controlling both linear axes (Figure 6.2c). Applying a dynamic modulation of the cutting depth (Figure 6.2d), with so-called tool servo technologies, further enhances the geometrical, and particularly the structuring, capabilities in ultra-precision turning (see next section). Examples of diamond-turned functional surfaces include Fresnel lenses [17], and, in the case of fast tool servo turning, faceted mirrors and micro lens arrays [18].

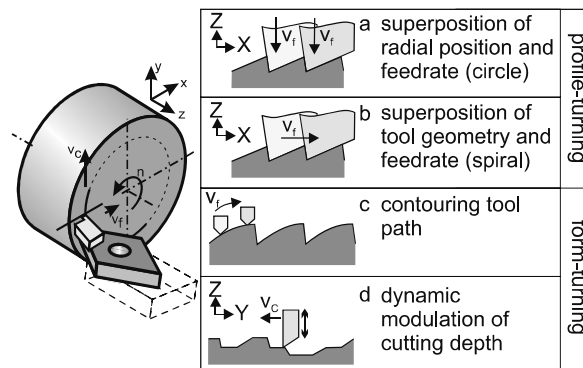


Figure 6.2 Principle of diamond turning and kinematic variations for structure generation

The inherent advantage of turning operations is the high machining speed, since the process time is scaling only linearly depending on the diameter of the workpiece. The constraints of diamond turning are mostly the kinematic roughness (i. e., influence of feed and tool nose radius), the dynamic machine performance, as well as the intrinsic material response.

Structures without rotational symmetry can be produced by turning operations when the cutting depth is dynamically modulated according to the radial and angular position on the surface (Figure 6.2d). Depending on the frequency of the modulation and the applied device, these processes are called slow slide, when using the machine tool's own slides, or fast tool servo turning, when specific accessory devices are used. In both cases—slow slide and fast tool servo—the devices are operated in a master-slave configuration, usually with the main spindle ruling the machining process.

The fast tool servo (FTS) concept was originally conceived for increasing the accuracy of an ultra-precision lathe [18] and was applied later for the non-circular turning of aspheres with a small deviation from rotational symmetry [2, 19]. FTS machining has been widely applied to manufacture micro components and complex micro structured surfaces such as micro prisms, lens arrays, torics, and off-axis aspheric surfaces with high accuracy and cost effectiveness [20]. The depth of cut is modulated dynamically according to the radial and angular position of a cutting tool on the workpiece surface (see Figure 6.2d). The high shape accuracy of cutting tools as well as the high resolution of synchronous multi-axial motion in ultra-precise machine tools are key advances in achieving the high surface and structuring qualities required. According to the drive mechanism of actuators, FTSs can be classified into hydraulic FTSs, piezoelectric FTSs, magnetostrictive FTSs, Lorentz force FTSs, and electromagnetically-driven FTSs. These systems have strokes from several micrometers to a few millimeters with frequencies from 20 Hz to 23 kHz [21].

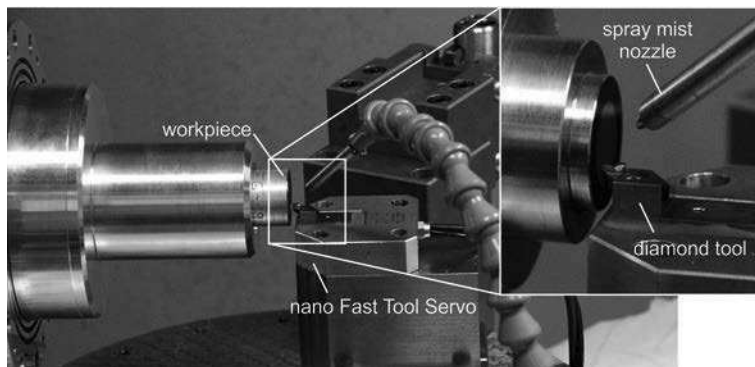


Figure 6.3 Machine set-up for diamond turning with a nano fast tool servo

FTS systems have been further developed for dedicated operations and structuring applications. Brinksmeier et al. [22] developed the nano fast tool servo (nFTS), featuring a stroke of up to 500 nm at a bandwidth of 5 kHz and higher (see Figure 6.3). The designed nFTS can generate a variation of the undeformed chip thickness within the nanometer range. This enables the processing of diffractive micro structures by combining a classical diamond turning process with a nano fast tool servo unit with a positioning accuracy of 4 nm. For the machining of blaze (saw tooth-shaped) structures, diamond tools with a knife geometry are used (see Figure 6.4). Due to this tool geometry and tool servo technology, it is possible to generate 2000 structure elements per revolution, each at an individual height level. Thus, it is possible to machine diffractive optical elements (DOEs) like holograms, in a single step process with sub-micron precision and optical grade surface roughness ($S_a < 10$ nm) [23]. These parts can be used directly as reflective metal optics [24] or applied as mold inserts for injection molding [25], see Section 6.4.3.

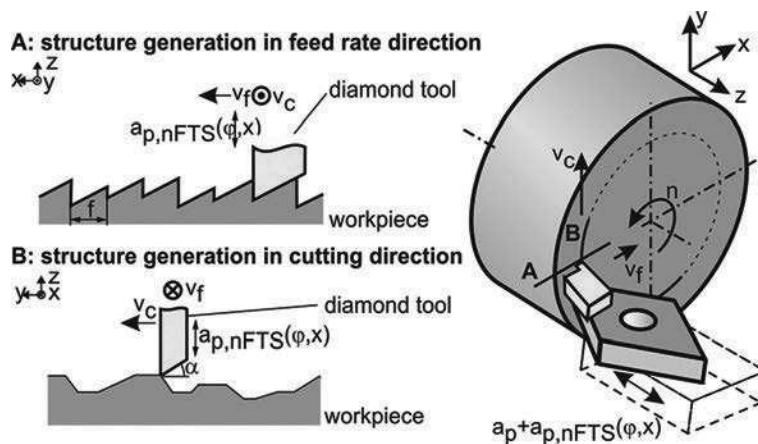


Figure 6.4 Working principle of the nano fast tool servo

End-fly-cutting-servo (EFCS) systems feature four-axis servo motions that combine the concepts of a fast/slow tool servo and end fly-cutting (see Section 6.2.2). A variety of nano structures can be generated with high accuracy (as a secondary structure on free-form surfaces or micro aspheric arrays), which is conventionally difficult to achieve. The method is useful to generate hierarchical micro nano structures [26].

The virtual spindle-based tool servo (VSTS) diamond turning method is capable of generating discontinuously structured micro optics as arrays by a fast or slow tool servo, greatly increasing the feasibility for machining discontinuous arrays of micro optics on both planar and free-form surfaces [27]. A virtual spindle axis is defined at a specific position by combining the translational and rotational servo

Considering its effect on the quality of the molded parts and on the process, the main advantages of vacuum-assisted micro injection molding can be summarized as follows:

- reduction of cavity backpressure due to air entrapment and consequent reduction of flow resistance (i. e., lower injection pressure) [2, 18]
- elimination of burn marks, due to the diesel effect, especially on knit lines and in corners or flanges opposite to the gate [19]
- absence of air bubbles and voids in the moldings [12, 20]
- better mechanical properties, especially at weld lines, where the interference of air with the two welding melts can reduce the part strength while also forming v-notches on the surface of the molded part that act as a stress concentration during the part's end-use [1, 2, 16]
- improved process control, e. g., shorter filling and cooling times, lower packing pressure [15]

Moreover, evacuation of air from the cavity before injection of the polymer melt can also yield some benefits for the tool [16]:

- reduction of tool erosion and consequent reduction of mold maintenance
- less buildups of volatiles in the cavities
- no need for periodical cleaning of venting slots

The limitations and issues arising when adopting vacuum-assisted micro injection molding can be summarized as follows:

- need to implement an active venting system, which means higher investments, increased complexity for process control, and maintenance difficulty [19]
- increased cycle time [1]
- decrease of cavity air compression and consequent reduction of mold temperature [17]

■ 8.3 Equipment and Design Solutions

8.3.1 Active Venting

The evacuation of air from the cavity in vacuum-assisted micro injection molding is performed by means of an active venting circuit [1]. Compared to conventional injection molding, air is not displaced by the advancing melt flow front pushing the air out of the cavity from either the parting plane, the ejector pins, or some slots machined for the purpose (i. e., passive venting). Instead, a pressure gradient is artificially created by means of a vacuum system connected to the molding tool.

The structure of an active vacuum system is shown schematically in Figure 8.2. The main elements of the circuit are the vacuum pump, the connecting/inlet elements, and the vacuum measuring device [1]. Vacuum pumps used for vacuum-assisted micro injection molding are usually mechanical systems that exploit a rotary device to remove gas molecules from the sealed volume. They usually work with nominal pumping speeds up to $1600 \text{ m}^3 \text{ h}^{-1}$, and the ultimate cavity pressure they could yield ranges from 0.05 to 20 mbar [21].

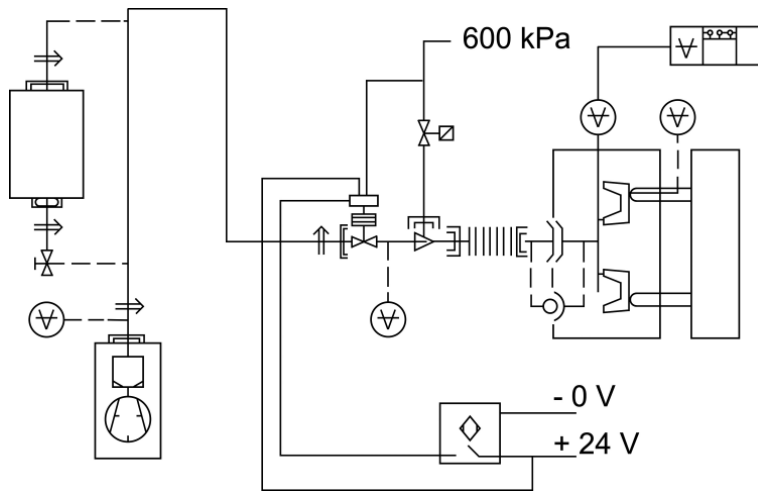


Figure 8.2 Vacuum system schematics, adapted from [1]

8.3.2 Mold Design for Vacuum-Assisted Micro Injection Molding

In vacuum-assisted micro injection molding, when designing the mold, the presence of some elements that allow the active evacuation of air from the cavity needs to be considered. The main elements that a mold for vacuum-assisted micro injection molding should include are the following:

- connecting elements for the vacuum pump
- venting channels to aspirate the air from the cavity
- vacuum inlets, placed at the end of the venting channel in the cavity or close to it
- sealing elements to allow the achievement of vacuum conditions inside the mold cavity

A typical design of molds for manufacturing micro- or nano-structured surfaces by micro injection molding is characterized by having the cavity in the moving half and the micro- or nano-structured interchangeable insert in the fixed mold half. For this reason, the main elements used to realize vacuum venting are included in

the moving half. However, different design solutions can be adopted to place the venting channels into the mold and to create a vacuum in the cavity through the inlet elements.

Venting channels can be included in the mold assembly by creating circular holes through the assembly, which reach the parting plane where they are connected to the venting inlets. With this design solution, some slots are usually machined in the cavity, as opposed to the injection location, as shown in Figure 8.3(a). When applying vacuum venting, the evacuating air flows outside from the cavity through these slots, which convey it into some channels that eventually lead to the venting channels (Figure 8.4(a)).

Alternatively, the elements connecting the vacuum pump and the venting inlets can be directly located inside a protrusion of the main cavity, as indicated in Figure 8.3(b). This is significantly thinner compared to the cavity substrate, and can then be easily trimmed from the micro-molded part. Despite being technically easier, this solution might not be acceptable for parts demanding high quality. However, as shown in Figure 8.4(b), the venting channels are significantly smaller and minor modifications of the conventional micro injection molding mold allow the application of vacuum venting.

In both cases, when designing the mold, the presence of an O-ring to seal the parting plane should be contemplated. The venting inlets are placed within the sealed area, thus are able to efficiently evacuate air from the cavity. However, when the venting channels go through the moving half of the mold assembly, more sealing elements should be located between each plate to guarantee a complete isolation of the venting inlets.

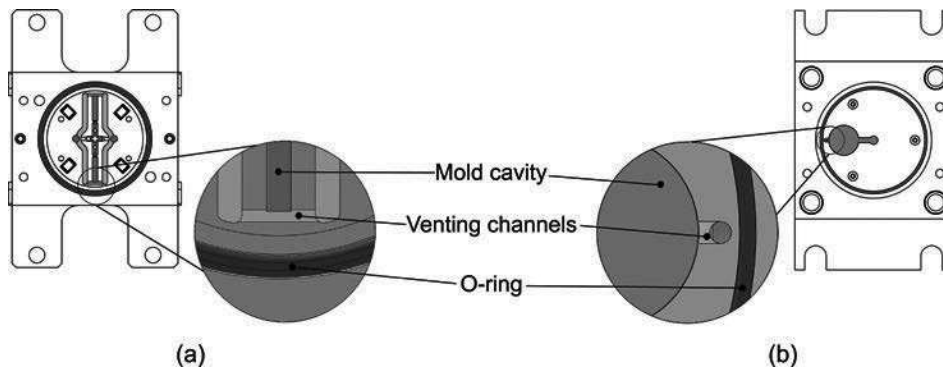


Figure 8.3 Venting channels machined (a) in the mold assembly and (b) in the cavity plate

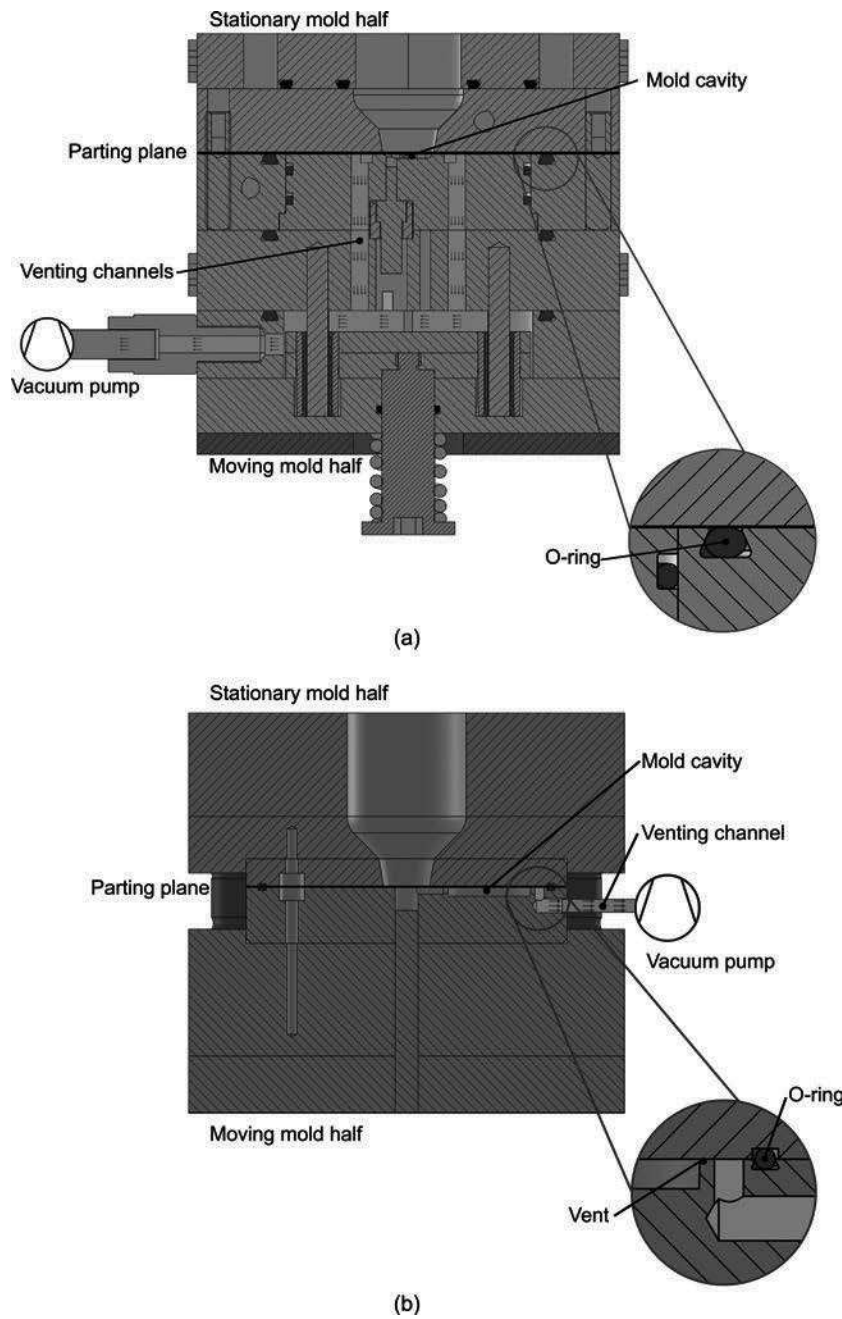


Figure 8.4 Mold design for vacuum-assisted micro injection molding with venting channels machined (a) in the mold assembly and (b) in the cavity plate. Different solutions for O-ring positioning are also shown

- predicting and improving the part quality, for example morphology and properties,
- gaining a better understanding of the process characteristics, and
- visualizing the process and inspecting the final product for, for example, possible air entrapment, warpage and shrinkage, weld lines, and so on.

In conclusion, simulations are widely applied and accepted in the plastics industry as helpful and efficient tools. Due to the complexity of the injection molding cycle, the equipment, and the materials used, as well as the requirement of an increase in the quality of the parts, process simulations of injection molding are indeed very attractive and relevant, and are gaining more attention. Process simulations in the plastic injection molding area have, in fact, been established for decades and are common practice in the plastics industry. Because of the rising number of applications of micro injection molded components, the interest and demand for reliable and supportive simulations in this area are increasing rapidly. Hence, simulation tools and related modeling must be addressed to fully develop the potential of micro injection molding [20, 22–25].

Nonetheless, carrying out simulations also comes with some drawbacks. It must not be forgotten that the underlying models usually incorporate idealizations, approximations, and assumptions—no matter how realistic or accurate the results might appear. In addition, the underlying model must be understood and there must be evidence to believe in the applicability and validity of the model independent of how good the real data are reproduced [11].

This chapter will give some insight into the modeling and simulation of the micro injection molding process, into what is currently feasible and investigated in this area, and into where possible limitations and pitfalls arise.

■ 9.2 Mathematical Background

9.2.1 Viscosity of Plastics

During the filling phase, the plastic flows into the cavity driven by the applied pressure of the injection molding machine. Hence, the plastic's viscosity is of major importance during the filling. The viscosity mathematically links the applied shear rate to the shear stress that the fluid experiences.

Newtonian fluids show a strictly linear behavior, meaning the viscosity is independent of the shear rate. In contrast, polymers are non-Newtonian fluids and, therefore, the viscosity is a function of the applied shear rate. When polymers experience shear, two effects come into play, leading to a decrease in viscosity, the

so-called shear thinning effect: heat dissipation and the alignment of the polymer chains [26].

In order to mathematically describe the viscosity, the power-law model was introduced in the 1920s [18]. It is one of the simplest and most common models for non-Newtonian fluids. According to the power-law model, the viscosity η of a plastic melt depends exponentially on the shear stress γ and is given as [27]

$$\eta(\dot{\gamma}) = m \dot{\gamma}^{n-1} \quad (9.1)$$

where m is the viscosity at a shear rate of one reciprocal second and n is the power-law index, which are both data-fitted constants. Generally, $n \leq 1$ for plastic melts, which reflects the shear thinning effect. This model describes the viscosity of plastics well at high shear rates. Nonetheless, injection molding is not only a high shear rate process. The shear rate is highest at the wall of the mold and decreases toward the center of the fountain flow where the shear actually vanishes completely, and the polymer melt exhibits the so-called zero shear rate viscosity.

Consequently, the power-law model is insufficient. Instead, the Cross model is widely applied and is part of most simulation software [14]. This model describes the shear rate dependency of the viscosity over a wide range of shear rates very well, because it combines a Newtonian region at low shear rates with a power-law shear thinning region at higher shear rates [18]. The viscosity is mathematically given by the Cross model as [26, 28]

$$\eta(\dot{\gamma}) = \frac{\eta_0}{1 + \left(\frac{\eta_0 \dot{\gamma}}{\tau^*} \right)^{1-n}} \quad (9.2)$$

where η_0 denotes a zero shear rate viscosity and τ^* is the critical stress level at the transition between the Newtonian plateau and the power-law region, which is determined by curve-fitting. The term $1 - n$ describes the slope of the viscosity curve in the power-law region when logarithmically plotted versus the shear rate, with n being equal to the power-law index.

The applied viscosity model in the simulation software must also account for the temperature changes happening during the entire injection molding cycle. The concept of time-temperature superposition can also be applied to the viscosity. The core of the concept is to shift the known viscosity curve at a reference temperature along the time axis in order to gain the viscosity curve at any temperature that differs from the reference temperature. The shift factor is given by the Williams-Landel-Ferry (WLF) equation, which can also be applied to the zero shear rate viscosity of the Cross model to introduce the temperature. This step yields the Cross-WLF model with its zero shear rate viscosity given as [14, 28]

$$\eta_0(T, p) = D_1 \exp \left[-\frac{A_1(T - D_2 - D_3 p)}{A_2 + T - D_2} \right] \quad (9.3)$$

where A_1 , A_2 , D_1 , and D_3 are constants, T is the temperature, and $D_2 = T_0$ is the reference temperature. The viscosity is also dependent on the pressure as given in Eq. 9.4. In many simulations or material models, this pressure dependency is commonly neglected by assuming that $D_3 = 0$. The pressure dependency is, nevertheless, quite relevant, because the injection molding process often exhibits high injection pressures [14]. More models exist to describe the viscosity of plastics. Common examples, which will not be discussed in more detail in this work, are the simple Cross, Carreau, and the Carreau–Yasuda models, which are described in other literature [27, 29]. Microscale viscosity is possibly an important aspect for the accurate modeling of micro injection molding. More details on this phenomenon and its relevance are described in Section 9.4.3. However, the currently available simulation tools do not consider microscale viscosity.

Moreover, semi-crystalline polymers show a sudden and significant increase in viscosity at their melting temperature due to the incipient formation of crystalline domains inside the materials. The aforementioned models do not undergo this viscosity increase due to crystallization [18]. Additionally, the micro structure of the final micro part might differ from a macro part, as micro injection molding causes higher shear rates and a different cooling and solidification behavior of the melt. The modeling of crystallization, and thus its impact on the mechanical characteristics of plastic parts, is a current topic of research. It is not yet fully integrated in any commercially available simulation software.

9.2.2 Thermodynamics

Besides the viscosity, information about the thermodynamic properties of materials is necessary for computer simulations of the injection molding process. This can be derived from the equation of the state of the material, which links the pressure, the specific volume (the inverse of the density), and the temperature. It is, therefore, also called pvT data [18].

For plastics, the data are usually provided as pvT diagrams, which show the specific volume v as a function of the pressure p and the absolute temperature T . The commonly used model for describing the curves of such a diagram is the two-domain Tait model, which is mathematically given as [30, 31]

$$v(p, T) = v_0(T) \cdot \left[1 - C \ln \left(1 + \frac{p}{B(T)} \right) \right] + v_t(p, T) \quad (9.4)$$